Science of the Total Environment (2020) 134388

Contents lists available at ScienceDirect

Science of the Total Environment

journal homepage: www.elsevier.com/locate/scitotenv

Unraveling long-term changes in lake color based on optical properties of lake sediment

Yihua Xiao [a,b,*], Thomas Rohrlack [b], Gunnhild Riise [b]

[a] Department of Biological and Environmental Science, University of Jyväskylä, FI-40014 Jyväskylä, Finland
[b] Faculty of Environmental Sciences and Natural Resource Management, Norwegian University of Life Sciences, NO-1432 Ås, Norway

HIGHLIGHTS

- In the studied lake, colored DOM represents a major proportion of sediment DOM.
- Recent lake color (2015) is four times browner than the period of 1800 to 1915.
- Terrestrial DOM dominated sediment DOM during the whole period (1800 to 2015).
- In-lake source of DOM has markedly increased since 2000.
- Lake browning is a result of multiple drivers varying in strength over time.

GRAPHICAL ABSTRACT

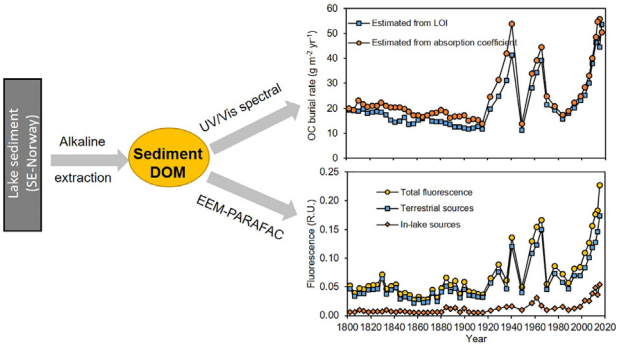

ARTICLE INFO

Article history:
Received 11 April 2019
Received in revised form 6 September 2019
Accepted 8 September 2019
Available online 09 September 2019

Editor: Ashantha Goonetilleke

Keywords:
Lake color
Sediment
Dissolved organic matter
UV-Vis spectroscopy
EEM-PARAFAC

ABSTRACT

A number of boreal surface waters have become browner over the last two decades. Recovery from acid rain is regarded as an important driver for this lake color increase, indicating a general browner lake color in preindustrial times. However, the lack of long-term monitoring data makes it challenging to unravel historical changes in lake color. In this study, we estimated long-term development in lake color (1800 to 2015) based on the optical properties of alkaline extractable dissolved organic matter (DOM) from sediment using UV–Vis and fluorescence spectroscopy. We found that the present lake color (2015) was significantly browner (four times higher in absorption coefficient) than for the period from 1800 to 1915 when lake color was at a lower and more stable level. Fluorescence excitation–emission matrices combined with parallel factor analysis (EEM-PARAFAC) indicate that terrestrially derived DOM was the main source of sediment DOM. However, the importance of in-lake source of DOM has significantly increased with time. The long-term trend in DOM burial was not consistent with the anthropogenic sulfur (S) deposition pattern. However, along with the increased sediment DOM, there has been increased precipitation, temperature and forest growth with time, which affect the production and degradation of DOM. Even though S deposition might have delayed the runoff of terrestrial DOM for a certain period, it comes in addition to other color-regulating factors. Thus, there is no single driver for the observed lake browning, but rather an interplay between different drivers varying in strength over time, such as afforestation, changes in areal use, declined S deposition, and increased temperature and precipitation.

* Corresponding author at: Department of Biological and Environmental Science, University of Jyväskylä, FI-40014 Jyväskylä, Finland
E-mail addresses: yihua.y.xiao@jyu.fi (Y. Xiao), thomas.rohrlack@nmbu.no (T. Rohrlack), gunnhild.riise@nmbu.no (G. Riise).

https://doi.org/10.1016/j.scitotenv.2019.134388
0048-9697/

1. Introduction

The browning of boreal surface waters over the last two decades is related to increased concentrations of dissolved organic matter (DOM) (Finstad et al., 2016; Roulet and Moore, 2006), which has profound effects on aquatic ecosystems. High concentrations of DOM can change water acidity, anoxic state (Knoll et al., 2018), light penetration depth (Karlsson et al., 2009), and biota (Nelson and Siegel, 2013). In addition, elevated lake color, caused by high concentration of DOM, affects societal water supply, since more effort is needed to produce high-quality (i.e., less colored) drinking water (Chow et al., 2007). The increase in DOM has been explained by a reduction in anthropogenic sulfur (S) deposition (Monteith et al., 2007), shifts in land use type (Finstad et al., 2016), variation in hydrology (Hongve et al., 2004; Köhler et al., 2013; Zhou et al., 2016), increased iron concentration (Kritzberg and Ekström, 2012), and climate change (Oni et al., 2013). Among these factors, a reduction in atmospheric S deposition has been assumed to be a main driver (Evans et al., 2012; Monteith et al., 2007; Valinia et al., 2015), indicating a higher DOM concentration in "preacidified" periods, as supported by sediment studies from Sweden (Bragée et al., 2015; Valinia et al., 2015). However, because long-term data (e.g., before 1950) are generally lacking, the underlying mechanisms and drivers for lake browning are still under debate. Recently, land use transition (Anderson et al., 2013; Kritzberg, 2017) and climate change (de Wit et al., 2015) have been proposed as the most important factors.

In order to track the long-term development of DOM in lakes, paleolimnological approaches can be very useful, e.g., Meyer-Jacob et al. (2017) and Renberg et al. (2009). Lake sediments are significant sinks of terrestrial organic matter (OM), globally, in its transport from land to sea (Cole et al., 2007a; Tranvik et al., 2009). Organic remains of both terrestrial and in-lake origins, preserved in chronological sequences, can serve as good proxies for lake water development in quantity as well as quality aspects of DOM (Saulnier-Talbot, 2016). Terrestrial DOM, which is recalcitrant and preferentially settles to the bottom, dominates in most boreal lakes (Gudasz et al., 2012; Guillemette et al., 2017). In contrast, in-lake source DOM, generated through biological and photochemical processes in lakes (Derrien et al., 2018; Torres et al., 2012) is generally more easily utilized and degraded.

Being convenient and sensitive techniques, both UV–Vis and fluorescence spectroscopy have been widely used to analyze the major fraction of DOM, chromophoric DOM (CDOM), in both water (Coble, 2007; Stedmon et al., 2003; Yamashita et al., 2015), soil- and sediment extracts (Derrien et al., 2017; Mielnik and Kowalczuk, 2018; Santín et al., 2009). Absorption coefficient in the visible range, for instance, at 410 nm, is highly correlated to the color and DOM in water (Hongve and Åkesson, 1996). Concerning properties of DOM, spectral slope coefficients (e.g., $S_{275-295}$) provide important information on the age and molecular weight (MW) (Helms et al., 2008), and absorption ratios such as E_2/E_3 and E_4/E_6 are good proxies for both MW and aromaticity of DOM (Cieslewicz and Gonet, 2004; Peuravuori and Pihlaja, 1997). Fluorescence analysis, combining fluorescence excitation–emission

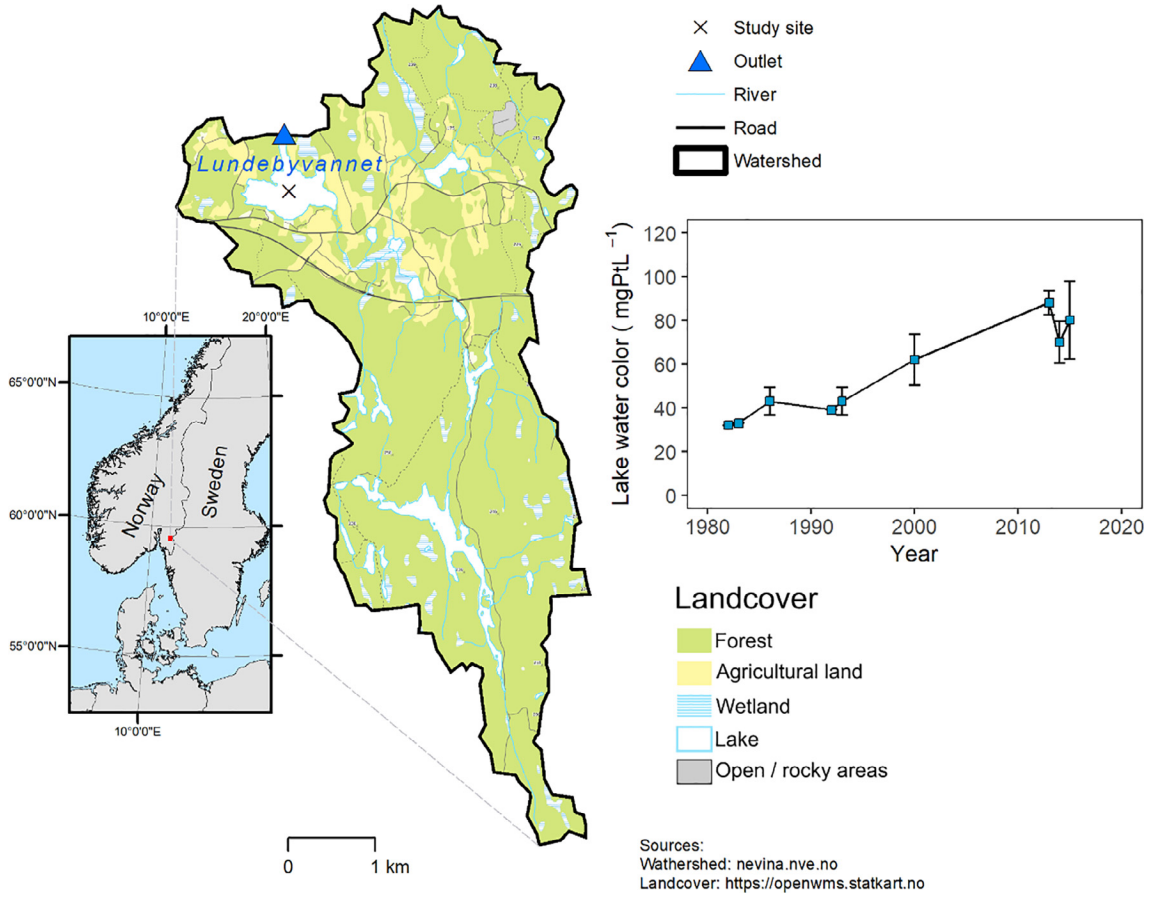

Fig. 1. The catchment of Lake Lundebyvannet and lake water color development from 1982 to 2015 (water color is calculated as the mean value from June to October of the year). Lake water color data is extracted from Norwegian Database on Environmental Quality (https://vannmiljofaktaark.miljodirektoratet.no/) and measured according to Norwegian Standard Association (1988).

Table 1
Water quality and morphometric characteristics of Lake Lundebyvannet.

Parameters	
Water characteristics[a]	
Color (mg Pt L^{-1})	119.2
TOC (mg L^{-1})	13.1
pH	6.2
TP (μg L^{-1})	27.3
TN (μg L^{-1})	612
Secchi (m)	1.3
Geographical characteristics[b]	
Area (km^2)	0.43
Max. depth (m)	5.5
Altitude (m)	158
Catchment area (km^2)	21.3
Forest (%)	78.9
Cropland (%)	10
Water (%)	6.4
Swamp (%)	4.1
Urban (%)	0.4

[a] Water characteristics were obtained from Hagman et al. (2015). TOC, total organic carbon; TP, total phosphorus; TN, total nitrogen. The variations in the development of TP and TN from 1982 to 2017 can be found in supplementary information Fig. S4.
[b] Geographical characteristics were extracted from Norwegian Water Resources and Energy Directorate (NVE, https://www.nve.no/).

matrices with parallel factor analysis (EEM-PARAFAC), allows for the independent estimation of different fluorescent components of CDOM, which give useful information on their sources and relative abundance (Kothawala et al., 2014; Stedmon and Markager, 2005).

This study was conducted in the downstream Lake Lundebyvannet, where lake color (mg Pt L^{-1}) has doubled between 1982 and 2017 (extracted from Norwegian Database on Environmental Quality, Fig. 1). Lake Lundebyvannet is located in a forest-dominated catchment (Fig. 1), below the marine level. Hence, clays make up an important part of the sediment material. In addition, there are agricultural activities and settlements in the vicinity of the lake, and Lundebyvannet serves as a popular recreation place for swimming. Recent surveys show that Lake Lundebyvannet does not satisfy the criteria for good ecological status set by the Water Framework Directive, mainly due to an excessive concentration of the nuisance microalgae *Gonyostomum semen* (Hagman et al., 2015). Thus, a multitude of factors might possibly affect the color of Lundebyvannet. In the present study, we estimated the long-term development of lake color and DOM, from approximately 1800 to 2015, by investigating the optical properties (through UV–Vis and fluorescence spectra) of alkaline extractable DOM from sediment, previously found to be a good representative of the bulk properties of the total sediment DOM pool (Hur et al., 2014). Here we assumed that sediment DOM was a good proxy for lake color development in the studied lake. By combining the optical properties of the sediments with events of importance for production and runoff of DOM, such as anthropogenic S deposition, changes in land use and climate (temperature and precipitation), key drivers for lake color development from a long-term perspective were identified. Based on lake sediment analyses, we aim to discriminate between different color drivers that vary in time and strength, which can provide useful input to future color development of boreal lakes.

2. Materials and methods

2.1. Sediment sampling and analyses

Two sediment cores (length 51 cm) were collected with an Uwitec sediment sampler in February 2017 from ice in the deepest part of Lake Lundebyvannet (59°32′57′N, 11°28′54′E), Eidsberg, southeastern Norway (Fig. 1). The chemical and geophysical characteristics of Lake Lundebyvannet are shown in Table 1. The sediment cores (6 cm diameter) were divided into layers of 1 cm thickness (51 sub sediment samples) on site and transferred to plastic bags. In order to avoid the uncertainties caused by high water content in the upper layer, only data from the lowest 50 sub sediment samples (from 2 cm to 51 cm depth) are reported. The sliced sediment samples were freeze-dried, prior to further analyses in the laboratory.

Freeze-dried samples from sediment core 1 were subject to analyses of loss-on-ignition (LOI), chlorophyll *a* (Chl *a*) and S content, in addition to sediment DOM extractions. LOI was determined from gravity analyses, based on the difference in weight from dried sediment material (105 °C for 24 h) and sediment material ignited at 550 °C for 2 h. Sediment OC was estimated from LOI by assuming a constant relationship between LOI and OC, where 50% is carbon (Dean, 1974; Håkanson and Jansson, 1983; Heiri et al., 2001). Estimation of Chl *a* was based on Thrane et al. (2015). A validation of the method was included in the Chl *a* analysis for uncertainty estimations. Total S was determined in subsamples (0.3 to 0.5 g dry weight) that were acid decomposed (69% (W/W) sub-boiled nitric acid, 260 °C) in a MLS-MILESTONE UltraCLAVE III microwave digestion system, prior to inductively coupled plasma optical emission spectrometry (Optima 5300 DV, Perkin Elmer).

Freeze-dried samples from sediment core 2 were shipped to University College of London (England) for depth-time chronology analysis. In order to estimate the annual amount of sediment deposited, radioactive Cesium (^{137}Cs) and Americium (^{241}Am) were analyzed by direct gamma assay (Appleby, 2002; Appleby et al., 1986). This method aims to find two peaks representing the Chernobyl accident (1986) and the latest nuclear test in the atmosphere (1962/1963), respectively. In addition, radioactive lead (^{210}Pb) was analyzed, which allows the dating of the sediments deposited between 1900 and today. The results were used to develop a mathematical model that converts the distance from the sediment surface to time when the sediments were deposited (Appleby, 2002; Appleby and Oldfield, 1978).

2.2. Sediment DOM extraction

Sediment DOM was extracted from freeze-dried sediment samples using an alkaline solution based on a method by Wolfe et al. (2002). The sediment samples (0.1 g dry weight) were extracted with 10 mL of 0.5 mol L^{-1} NaOH in glass ampoule bottles (25 mL total volume). After closing the glass ampoule with a rubber cap that was sealed with an aluminum collar, the headspace of the ampoule was vacuumed and filled with pure N_2. The vacuumization and N_2 injection cycle were repeated five times to ensure that the headspace was pure anoxic. The extraction bottles were shaken for 24 h under dark conditions. To stop the extraction, the extracted solution was transferred to a 15 mL centrifuge tube and centrifuged for 10 min at 3000 rpm. Before optical analyses, the supernatant passed through a 0.7 μm filter (GF/F, Whatman) and neutralized to pH ~7 with HCl. In order to minimize inner filter effects during fluorescence measurements, the extracted solution was diluted 100 times (final concentration for absorption and fluorescent spectral measurements was 0.1 g dry weight L^{-1}) with Milli-Q water (Millipore) to make sure the absorbance at 254 nm (A_{254}) was <0.2 (Ohno, 2002).

2.3. UV–Vis spectral measurement

Spectral absorbance (A_λ) over the wavelength range of 200 to 700 nm was measured using a UV–Vis spectrophotometer (UH

5300, Hitachi). Absorption coefficient (a) at wavelength λ, a_λ (m^{-1}) was calculated by.

$$a_\lambda = 2.303 \times A_\lambda L \quad (1)$$

where L is the length of absorption path (L = 0.01 m).

In this study, we selected light absorption coefficient at a wavelength of 410 nm (a_{410}) as an indicator for water color (Hongve and Åkesson, 1996). Sediment dissolved OC (DOC) concentration was estimated by a_{410} using a linear regression model, DOC = 0.504 × a_{410} + 5.30 (r^2 = 0.722, n = 43, P < 0.05, provided by data from Lundebyvannet lake and catchment water, Table S2). The spectral slope coefficient was obtained by linear regression and calculated from the ln-transformed absorption coefficient using the wavelength range of 275 to 295 nm ($S_{275–295}$) and 350 to 400 nm ($S_{350–400}$). The spectral slope ratio (S_R) was calculated by dividing $S_{275–295}$ by $S_{350–400}$ (Helms et al., 2008). Absorption coefficient ratios of E_2/E_3 (calculated by the ratio of A_{250} to A_{365}) and E_4/E_6 (calculated by the ratio of A_{250} to A_{365}) are calculated as proxies of DOM MW and aromaticity (Cieslewicz and Gonet, 2004; Li and Hur, 2017; Peuravuori and Pihlaja, 1997).

2.4. Fluorescence spectra and PARAFAC modeling

Fluorescence excitation–emission matrices (EEMs) were scanned using a Cary Eclipse Fluorescence Spectrophotometer (Varian). The excitation wavelength (Ex) was set from 240 nm to 450 nm with a 5 nm increment, and the emission wavelength (Em) was from 300 nm to 600 nm at 2 nm interval. The slit width was set to 5 nm for both Ex and Em. The samples were scanned at 2400 nm min^{-1} with a voltage of 800 V. A blank EEM (Milli-Q, Millipore) with identical settings was measured every day. A Raman scan using Milli-Q water (Millipore) was collected daily for Raman normalization. The Raman scan used an excitation wavelength of 275 nm and recorded emissions at 1 nm intervals from 285 nm to 450 nm (Murphy et al., 2013).

A total of 50 raw EEMs were collected for PARAFAC modeling. Before running PARAFAC analysis, the 50 raw EEM datasets were fully corrected according to standardized procedures (Appendix A, Murphy et al., 2013). These corrections include spectral correction, background subtraction, inner filter effects correction, and Raman normalization. PARAFAC modeling was carried out in Matlab R2015b (Mathworks, USA) using the decomposition routines for Excitation Emission Matrices (drEEM) toolbox (version 0.3.0, http://models.life.ku.dk/drEEM). The data array was divided into four splits, each containing a quarter of the dataset. These four splits were combined in six different ways to generate six new halves. The PARAFAC algorithm will run stepwise on each half independently, yielding 3 to 7 components. Three split-half comparisons were tested. Finally, the number of the components was validated by split-validation using a Tucker congruence coefficient (TCC > 0.95). The procedure for PARAFAC modeling is well described by Murphy et al. (2013). The maximum fluorescence intensities (F_{max}, in Raman unit [R.U.]) of identified components were reported.

2.5. Temperature and precipitation data

Long-term (1874 to 2015) annual mean air temperature and precipitation of the studied area were obtained from the adjacent Field Station for Bioclimatic Studies (Source: https://www.nmbu.no/fakultet/realtek/laboratorier/bioklim/meteorologiske-data) in Sørås, Ås, Norway. The temperature and precipitation data are shown as aggregated mean data at the same time resolution (per 2–9 years) as the sedimentation rate data.

2.6. Statistical analyses

All statistical analyses were performed in RStudio 3.5.1 (2019–2018 RStudio, Inc). One-way ANOVA analysis was conducted to evaluate the significance difference between time series (1800–1915, 1915–1985, and 1985–2015) of individual variables. According to Shapiro-Wilk normality test (Royston, 1995), our data does not follow a normal distribution in periods of 1915–1985 (n = 11) and 1985–2015 (n = 9) because of low sample numbers. Therefore, Kruskal-Wallis nonparametric ANOVA was performed. The relationship between OC burial estimated by LOI and a_{410} was evaluated by Pearson correlation analysis using "cor" function of "stats" package. Simple and multiple linear regression analyses were conducted using function of "lm" of the "stats" package to evaluate OC burial explained by S, temperature, and precipitation. The significance level was set at P < 0.05. As all regression models were significant (P < 0.05), the goodnesss of fit was evaluated by using the coefficient of determination, r^2. Principal component analysis (PCA) of log-transformed selected variables was conducted by using "rda" function of "vegan" package. The PCA figure was plotted by using "ggplot2" function.

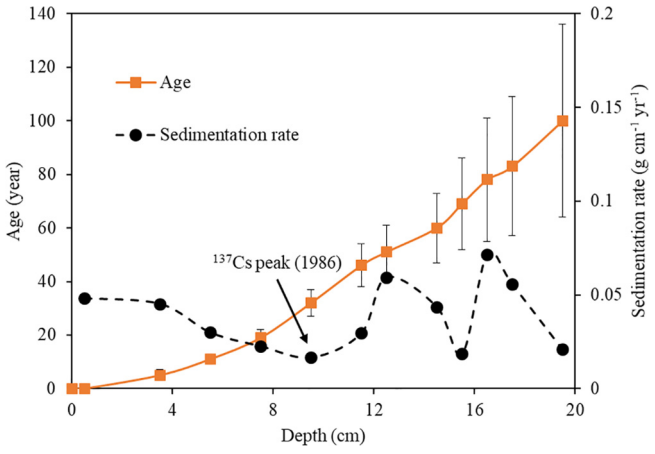

Fig. 2. Radiometric chronology of a core taken from Lake Lundebyvannet, Norway, showing ^{210}Pb dates and sedimentation rates based on the CRS-constant rate of ^{210}Pb supply model. The solid line shows age while the dashed line indicates sedimentation rate.

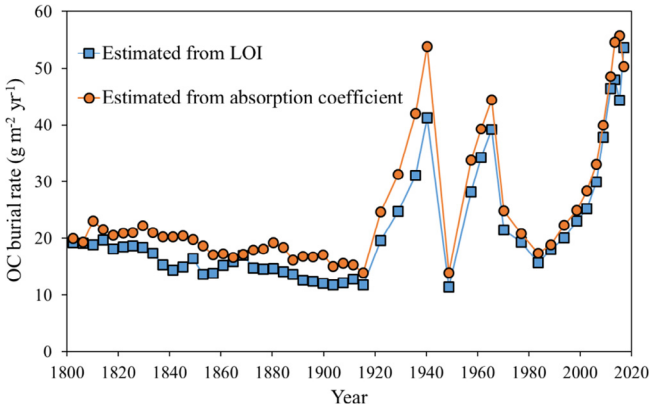

Fig. 3. Organic carbon (OC) burial rate estimated from loss on ignition (LOI, blue line) and absorption coefficients of sediment alkaline extractable organic matter (a_{410}, orange line, adjusted to sedimentation rate). (For interpretation of the references to color in this figure legend, the reader is referred to the web version of this article.)

Table 2
Variables (mean ± standard deviation) studied in the present study during three periods: 1800–1915 (n = 30), 1915–1985 (n = 11), and 1985–2015 (n = 9).

Year	1800–1915	1915–1985	1985–2015
OC burial (g m^{-2} yr^{-1})	15.4 ± 2.55[a]	26.0 ± 9.66[b]	32.5 ± 11.8[b]
Chl *a* (μg cm^{-2} yr^{-1})	2.08 ± 0.84[a]	5.38 ± 2.29[b]	13.3 ± 4.93[b]
a_{410} (m^{-1})	1.51 ± 0.44[a]	2.02 ± 0.72[a]	3.74 ± 1.59[b]
Fluor (R.U.)	0.05 ± 0.01[a]	0.10 ± 0.04[b]	0.13 ± 0.06[b]
C1 (R.U.)	0.018 ± 0.005[a]	0.040 ± 0.019[b]	0.050 ± 0.019[b]
C2 (R.U.)	0.012 ± 0.004[a]	0.027 ± 0.014[b]	0.032 ± 0.015[b]
C3 (R.U.)	0.007 ± 0.001[a]	0.014 ± 0.005[b]	0.022 ± 0.010[b]
C4 (R.U.)	0.005 ± 0.001[a]	0.009 ± 0.004[b]	0.014 ± 0.006[b]
C5 (R.U.)	0.003 ± 0.003[a]	0.006 ± 0.006[b]	0.016 ± 0.011[b]
(C1 + C2 + C3)%	83.8 ± 3.74[a]	83.2 ± 4.38[ab]	78.9 ± 3.98[b]
(C4 + C5)%	16.2 ± 3.74[a]	16.8 ± 4.38[ab]	21.1 ± 3.98[b]
$S_{275-295}$ (μm^{-1})	9.61 ± 0.28[a]	9.70 ± 0.32[ab]	9.30 ± 0.49[b]
S_R	0.82 ± 0.04	0.82 ± 0.04	0.81 ± 0.03
E_2/E_3	3.10 ± 0.12[a]	3.08 ± 0.14[a]	2.92 ± 0.04[b]
E_6/E_4	5.13 ± 0.69	5.16 ± 1.22	4.81 ± 0.74
Sulfur (mg S g OC^{-1})	6.76 ± 1.47[a]	21.2 ± 3.89[b]	18.6 ± 8.00[b]
Temperature (°C)	4.70 ± 0.68[a*]	4.92 ± 1.03[a]	6.33 ± 0.64[b]
Precipitation (mm)	568 ± 63.6[a*]	656 ± 67.7[a]	786 ± 100[b]

Fluor: total fluorescence of sediment DOM; (C1 + C2 + C3)%: the relative fluorescence intensity of terrestrial humic-like organic matter; (C4 + C5)%: the relative fluorescence intensity of in-lake source organic matter.
The significance analysis was performed with ANOVA. Different letters (a and b) represent significant differences (P < 0.05) between different periods.
[*] The sample numbers for temperature and precipitation from 1800 to 1915 are 10.

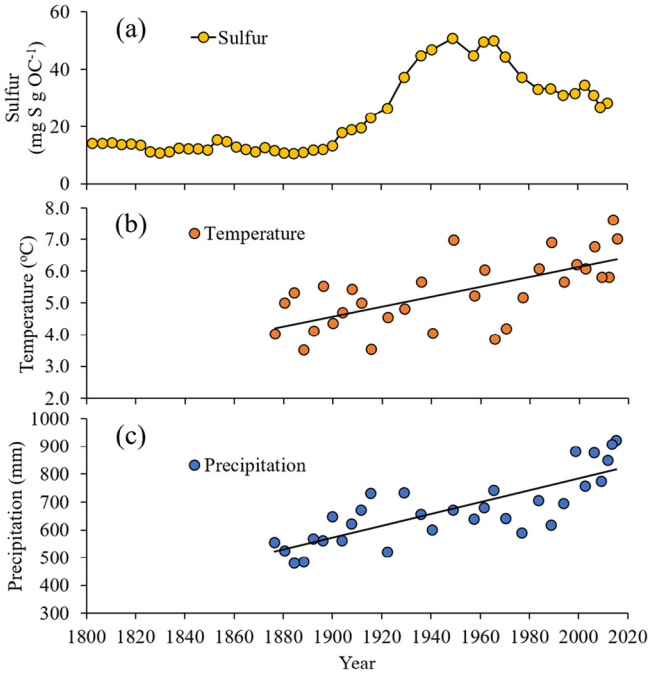

Fig. 4. Sulfur deposition in relation to organic carbon (mg S g OC^{-1}) in lake sediment (a), annual mean air temperature (b), and annual mean precipitation (c). The solid lines in (b) and (c) indicate the trendline from linear regression. Temperature and precipitation data were extracted from field station for bioclimatic studies – BIOKLIM at Sørås Field in Ås, Norway.

3. Results

3.1. Sediment dating

The results based on the ^{210}Pb dating model were in agreement with the ^{137}Cs Chernobyl peak for 1986 (highest value at a depth of 9.5 cm), indicating reasonable dating estimates for sediments deposited after 1915 (Fig. 2 and Table S1). In order to estimate the age of sediments deposited before 1915, we assumed that the sedimentation rate for the period from 1800 to 1915 was constant and at the same rate as in 1915 (0.021 g DW cm^{-2} yr^{-1}, Fig. 2). Therefore, the time estimates prior to 1915 are subject to some uncertainty, and should be treated with caution.

The sedimentation rate has generally increased in the two to three most recent decades (since 1990s, Fig. 2). Prior to this period there were two major peaks in sedimentation rate, one during the 1960s and the other during the 1940s. In between, a minimum sedimentation rate was found around 1950.

3.2. OC burial and UV–Vis spectra

OC burial rate in this study was estimated in two ways: from both LOI analysis ($OC_{burial\text{-}LOI}$) and absorption coefficient a_{410} measured by UV–Vis spectroscopy ($DOC_{burial\text{-}a410}$, Fig. 3). A high correlation between OC (or DOC) burial estimated by a_{410} and LOI was found (Figs. 3 and S1). The slightly higher OC burial rates obtained by the a_{410} method from 1800 to 1970 and after 2012, might be due to uncertainty in the conversion factors from both a_{410} and LOI to OC.

Based on the OC burial trends (Fig. 3), we divided the whole study period into three time periods, 1800–1915, 1915–1985, and 1985–2015 (Table 2). In preindustrial times (1800 to 1915), the OC burial rate was significantly lower (mean $OC_{burial\text{-}LOI}$ = 15.4 g C m^{-2} yr^{-1}, Table 2) compared to the burial rates after 1985 (mean $OC_{burial\text{-}LOI}$ = 32.5 g C m^{-2} yr^{-1}, Table 2). Irregular peaks in OC burial were found during the period from 1915 to 1985 (around 1940 and 1966, Fig. 3), followed by a lower OC burial period during the 1980s, and then a sharp increase up to recent years (Fig. 3).

Concerning the absorption coefficient a_{410}, it has significantly increased since 1915, in comparison with the relative stable period with low values during 1800–1915 (Table 2). In comparison with the early period from 1800 to 1915, the mean spectral slope coefficient $S_{275-295}$ and absorption ratio E_2/E_3 in the recent period (1985–2015) have significantly decreased by 3.2% and 5.8%, respectively (Table 2 and Fig. S2). No significant variation was found for the spectral slope ratio (S_R) and the absorption ratio E_4/E_6 during the whole study period (Table 2).

3.3. Fluorescence spectra and PARAFAC

The trends for total fluorescence are the same as OC burial and Chl *a* (Table 2 and Fig. S3a). In comparison with the period of 1800–1915, the mean fluorescence intensities of the periods of 1915–1985 and 1985–2015 have significantly increased (ANOVA analysis P < 0.05, Table 2). Five fluorescent components were identified from the EEM-PARAFAC model, of which four were humic-like components (C1, C2, C3, and C5; Ex/Em: 260/510, 250(310)/420–430, 255(355)/432, and 320/384, respectively) and one was protein-like component (C4; Ex/Em: 270/314). The spectral loadings and intensities over time of the five PARAFAC components can be found in Figs. S3b and S3c.

In comparison with the published PARAFAC components in the OpenFluor database (Murphy et al., 2014), these five components have been reported in previous freshwater and sediment studies (Bittar et al., 2015; Hur et al., 2014; Kothawala et al., 2014; Lapierre and Del Giorgio, 2014; Zhang et al., 2009). The actual fluorescence intensities of all five components have significantly increased since 1915 in comparison with the period 1800–1915 (Table 2 and Fig. S3b). The fluorescence intensity of the terrestrially derived humic-like DOM (sum of C1, C2, and C3), followed exactly the same pattern as total fluorescence (Fig. S3a). The relative mean intensity (78.9% of total fluorescence) of terrestrially derived DOM

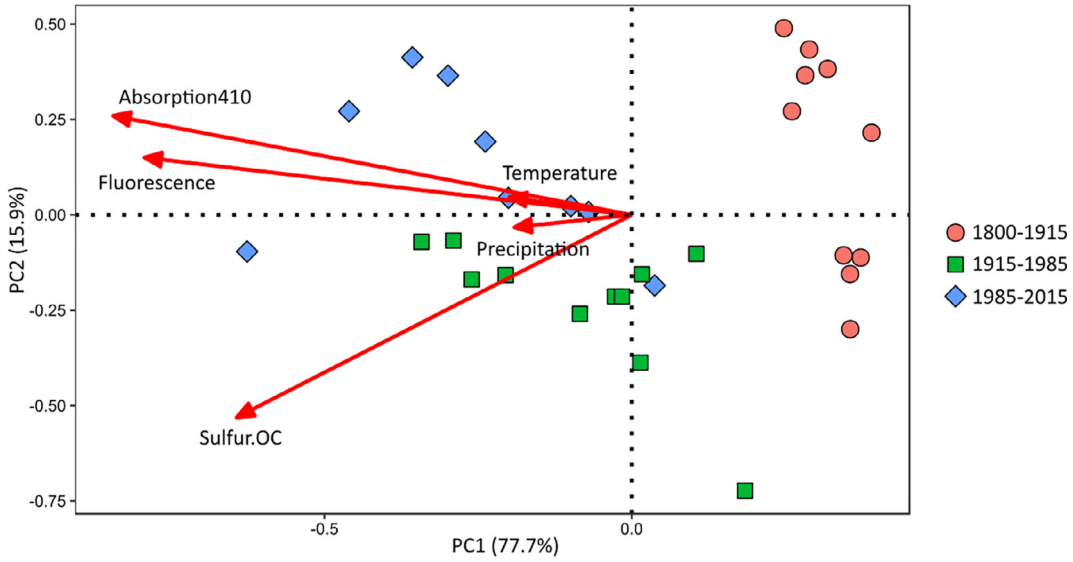

Fig. 5. Principle component analysis (PCA) of selected variables. "Absorption410" represents the absorption coefficient of sediment DOM at 410 nm. "Sulfur.OC" represents sulfur deposition in relation to organic carbon (mg S g OC^{-1}).

Table 3
The estimated coefficients and the coefficients of determinations (r^2) for the simple and multiple linear regression models of organic carbon burial (OC_burial) explained by sulfur deposition in relation to organic carbon (S, mg S g OC^{-1}), temperature (Temp), and precipitation (Precip).

Model	Model equation	r^2	*n*
1	OC_burial = **0.870** S + **10.3**	0.467	50
2	OC_burial = **6.26** Temp – 9.46	0.321	30
3	OC_burial = **0.070** Precip – **23.3**	0.481	30
4	OC_burial = **0.730** S + **3.98** Temp – 9.00	0.517	30
5	OC_burial = **0.549** S + **0.050** Precip – 18.1	0.573	50
6	OC_burial = **3.03** Temp – **0.056** Precip – **29.4**	0.535	50
7	OC_burial = **0.490** S + **2.41** Temp +**0.040** Precip – **23.5**	0.606	50

The coefficients significantly differing from zero ($P < 0.05$) are marked in bold. All models are significant with $P < 0.05$.

(humic-like components, C1, C2, and C3 together) of period 1985–2015 has significantly decreased in comparison with the period of 1800–1915 (mean of 83.8%, Table 2). In contrast, the actual and relative intensity of two in-lake source related components (protein-like C4 and microbially derived C5) have significantly increased by comparison with the recent period of 1985–2015 to the period of 1800–1915 (Table 2 and Fig. S3a). Please note that component C5 was also found in agricultural catchments (Wilson and Xenopoulos, 2009), indicating that C5 can be produced from both in-lake processes (Kothawala et al., 2014) and agricultural soil run-off from catchment (Wilson and Xenopoulos, 2009).

3.4. Drivers for lake color

The S content in the sediment samples has significantly increased in relation to OC since the 1900s along with increased industrialization and anthropogenic S deposition, peaking around 1950 to 1970 and then starting to decrease (Table 2 and Fig. 4a). S content in the sediment from 2012 (28.3 mg S OC^{-1}) returned to a similar level as in 1922 (26.5 mg S OC^{-1}). There was no direct relationship between the S deposition trend and OC burial in the sediment. For example, a dramatic change in OC burial were found during 1940–1960 at a time when S deposition was maintained at a relatively high level (Figs. 3 and 4a).

The trends of mean air temperature and precipitation, with the same time resolution as the sediment slicing (1 cm layers), are shown in Fig. 4b–c. The mean annual air temperature and precipitation over the whole period was 5.4 °C and 663 mm yr^{-1}, respectively. Significant increases in mean temperature and precipitation were found for the period 1985–2015 in comparison to earlier times in 1800–1915 (Table 2). Thus, the studied area is exposed to a much warmer and wetter climate today than in previous years.

PCA analysis of selected variables shows that PC1 and PC2 explain roughly 94% of the variability in the data with most variance explained on PC1, where the younger sediments (period of 1985–2015), generally were located to the left, the older sediments (period of 1800–1915) to the right, and the middle period 1915–1985 in between (Fig. 5). PCA Loadings for precipitation, temperature, and S in relation to OC clustered together with sediment absorption (at 410 nm) and fluorescence signals (Fig. 5). From simple and multiple linear regression analyses, we found that temperature, precipitation, and S in relation to OC are all major determinants of OC burial, of which annual mean precipitation alone best explains (48.1%) OC burial followed by S deposition in relation to OC (41.0%) and annual mean temperature (32.1%, Table 3). Precipitation, temperature, and S in relation to OC together explain 60.6% of the OC burial in the studied lake sediment (Table 3).

We have no good proxy for areal use in the PCA plot, so the variablity that is not explained (6%) might partly be related to changes in areal use. Although, specific land use history in the area is missing, old maps (https://www.kartverket.no/kart/historiske-kart) indicate agricultural activities for the whole study period, from 1800 until now. Air-photos from the Lundeby area also show that peat areas have been drained in previous time. Peat extraction activities were much more common in the past. The production of roast peat was at its highest during World War II (1940–1945), while the use of peat as soil amendment was peaking after 1960s (Lie, 2002). Large changes have also occurred within agriculture and forest production in newer times. Since 1950, agricultural cultivation of eastern Norway have been altered to grow almost exclusively grain, which has required diching and levelling for efficient food production (Stabbetorp, 2014). Concerning forestry, the standing volume of forest in southeastern Norway has significantly increased since the 1910s according to the Norwegian Inventory Forest Survey (Granhus et al., 2012).

4. Discussion

4.1. Optical properties of sediment DOM and OC burial: variation over time

The burial rates of OC estimated from a_{410} and LOI follow each other closely, indicating that colored DOM (i.e., CDOM) makes up a major proportion of alkaline extractable DOM from the sediments (Figs. 3 and S1). The results for fluorescence follow a similar pattern, indicating that terrestrial DOM (C1 + C2 + C3) makes up as much as 78.9% to 83.8% of sediment DOM (Fig. S3a and Table 2). This finding is consistent with previous studies, showing that lake DOC is mainly regulated by terrestrial DOM, a fraction of DOM that is preferentially preserved in the sediments (Chmiel et al., 2015; Cole et al., 2007b; Guillemette et al., 2017). The high correlation between OC burial estimated from a_{410} and LOI (Fig. S1), verify that the alkaline extraction efficiency of DOM for spectroscopic analyses is high, up to 100% for some periods. Periods when OC burial was uncoupled from a_{410} and LOI indicate uncertainties in the conversion factors from both a_{410} and LOI to OC or burial of non colored material (Fig. 3).

Differences in terrestrial delivery of OC to the lake, results in large variations in the settling of OC over time (Fig. 3). For a long period (1800 to 1915, Fig. 3), there was a constant trend in OC burial with time, indicating relatively stable conditions with few disturbances in the catchment. The period from 1915 to 1985 was, however, characterized by large fluctuation, probably reflecting changes in agricultural activities, for instance, ditching and levelling (Stabbetorp, 2014), drainage of wetlands or peat production (Lie, 2002), affecting the transport of sediments, including OC. After the fluctuating period of 1915–1985, a recent sharp increase in OC supply was found from 1985 to 2015 (Fig. 3 and Table 2). Monitored lake color of Lundebyvann from 1982 to 2017 is in line with the recent increase in DOM, as the water color (mg Pt L^{-1}) has doubled since the 1980s (Fig. 1), a finding which is in agreement with several other studies from the Northern Hemisphere (Arvola et al., 2010; Monteith et al., 2007; Weyhenmeyer et al., 2014).

During the earliest period, with constant OC burial and color (a_{410}) over time (1800–1915), there were generally small variations in properties of DOM (Table 2 and Fig. S3), shown by spectral slope coefficients ($S_{275-295}$) and absorption ratios (E_2/E_3), serving as good proxies for the MW and aromaticity of DOM (Helms et al., 2008; Peuravuori and Pihlaja, 1997). Along with changes in burial rate, the properties of DOM also changed with time. Significant decreases in means of $S_{275-295}$ and E_2/E_3 of period 1985–2015 compared to the means of 1800–1915, suggest that the MW and aromaticity of DOM have significantly increased for the most recent period. In between (1915–1985), there were large fluctuations in both $S_{275-295}$ and E_2/E_3, indicating variation in the source material of DOM and more instability in the terrestrial delivery of DOM. Increases in DOM are often related to the mobilization of "old" DOM (Guo and Macdonald, 2006), which likely has a higher aromaticity and stability against degradation compared to more newly produced DOM. Thus, during periods with enhanced DOM levels, "old terrestrial pools" with stored OC might be mobilized, whose accessibility is probably very water level dependent, attributing to large fluctuations as observed during the period 1915–1985.

Use of sediments as historical archives, assumes well preservation of DOM after burial in the lake sediments. During the transport of DOM from the terrestrial catchment to the lake bottom, several photo- and biodegradation processes occur, leaving a more recalcitrant DOM fraction behind (Attermeyer et al., 2018; Hansen et al., 2016; Lambert et al., 2016). This suggests that buried OM is relatively stable and its diagenetic transformation (e.g., postdepositional degradation) is small, as found by Chmiel et al. (2015). Anoxic conditions in the sediment pore water contribute to a preservation of OM (Maerki et al., 2006; Sobek et al., 2009). In addition, high sedimentation rates of mineral matter (clay), which is the case for the Lundeby lake, promote rapid burial and conservation of OM (Yu et al., 2009). Aromaticity is a good proxy for the diagenetic status of sediment DOM (Chen and Hur, 2015). The significant higher aromaticity (observed as a decrease in absorption ratio E_2/E_3) in recent years (1985–2015) compared to the old period of 1800–1915 also support high preservation of DOM and low degree of diagenetic transformation within this limited study period (app.200 year), in a geological time setting.

4.2. DOM quantity and quality and its main drivers

The variation of S deposition in relation to OC in the Lundebyvannet sediment (Fig. 4a) match well with the atmospheric S deposition modelled for the neighboring country - Sweden between 1880 and 2010 (Moldan et al., 2013). This suggest that the S pattern in the studied lake sediment can be a good estimate for the anthropogenic S deposition during the acid rain period. Many studies have proposed that atmospheric anthropogenic S deposition is a key driver for the recent DOM increase in surface waters (Evans et al., 2012; Monteith et al., 2007; Valinia et al., 2015). Declined atmospheric S deposition promotes increased molecular charge (Kalbitz et al., 2000) and reduced ionic strength (de Wit et al., 2007), which increase the mobility of DOM from the terrestrial catchment. In the present study, we find a significant positive relationship between S content and OC burial (Model 1, Table 3). Thus, in the long run, there is no inverse relationship between S deposition and OC burial, that can explain the recent DOM levels which are much higher than in preindustrial times (Figs. 3 and 4a). A finding that is supported by Kritzberg (2017), which suggests other important DOM drivers than anthropogenic S deposition.

Land use changes, which include activities related to agriculture and afforestation, affect the storage and leaching of DOM, that obviously can change the terrestrial supply of DOM and lake color (Anderson et al., 2013; Wilson and Xenopoulos, 2009). Agricultural activities in the Lundeby area have changed considerably from the early signs of development in 1775 with traditional farming to the recent, more intensive production. In particular, the conversion from grass to grain cultivation since the 1950s and the consequent increase in fertilizer application along with prolonged periods of open fields exposed to erosion affect sediment transport to the lake. A two-fold increase in grain production has occurred since the 1940s (Rohrlack and Haaland, 2017). Increasing fertilizer application is frequently followed by a rise in nutrient and DOM export to waters (Carpenter et al., 1998; Soranno et al., 1996), which might have impacted the supply of DOM after 1915, and especially after 1950 (Fig. 3). During the recent 30 years, there are large annual variations in the nutrients nitrogen and phosphorus (P), although there seems to be a gradual increase in P (Fig. S4).

Even though the intensity of agricultural production have increased, the total agricultural area in Eidsberg municipality has decreased by 20% from 1907 to 2016 (Rohrlack and Haaland, 2017), followed by increased forest coverage, which is known to affect DOM export (Finstad et al., 2016; Guay et al., 2014; de Wit et al., 2015). Surveys from the Norwegian National Forest Inventory shows that the standing volume of forest in eastern Norway, as for the whole of Norway, has steadily increased since the 1910s (Granhus et al., 2012). Even though there is no specific forest data for the Lundeby catchment, recent satellite images from the area compared with older pictures from 1775 and 1913 show increased density of trees (Rohrlack and Haaland, 2017). It is reasonable to assume that increased forest growth has contributed

to increased terrestrial supply of DOM to the lake since the 1910s, as observed as an increase in terrestrial fluorescent DOM (C1 + C2 + C3) after 1910s (Fig. S3a). Aerial photographs also show that the catchment area has been used for peat extraction (http://www.kartverket.no/kart/historiske-kart), which has a large impact on the turnover and leaching of organic carbon. Especially during periods of artificial draining and natural rewetting after dry periods, the supply of DOM from the peat areas is assumed to be high. All these together may explain the large OC burial fluctuations from 1915 to 1985 (Fig. 3).

Climate (i.e., temperature and precipitation) has clearly changed during the study period (Fig. 4b–c), becoming much warmer and wetter, as observed in neighboring Sweden and also globally (Bragée et al., 2015; Pilla et al., 2018). In addition to increased forest growth, increased temperature contributes to increased primary production in the lake (e.g. Wilson and Xenopoulos (2009)). Along with enhanced nutrient supply (Fig. S4), this rise in temperaure enhance the importance of in-lake sources and their contribution to DOM, supported by an increase in protein-like (C4) and microbially derived DOM (C5) from a mean of 16% during 1800–1915 to 21% during 1915–2015 (Table 2). The similar trends of OC burial and Chl *a* also supports the recent impact of primary production to DOM development in the studied lake (Table 2). In addition, increased precipitation also increase the terrestrial export of DOM to waters (Evans et al., 1988; Haaland et al., 2010; Hongve et al., 2004), as observed as an increase in the relative fluorescence of terrestrial DOM (C1 + C2 + C3, Table 2 and Fig. S3a), and a positive correlation between OC burial and precipitation ($r^2 = 0.481$, Table 3).

5. Conclusions

Based on the optical properties of sediment DOM, using UV–Vis and fluorescence spectroscopy, long-term changes in lake color and its main drivers have been elucidated. The consistency of OC burial calculated from LOI and the absorption coefficient demonstrate that the optical approaches used in this study are valid. Overall, the combined optical properties of sediment DOM with other chemical and biological proxies (OC, S, and Chl *a* burial), in addition to changes in land use and climate, indicate that there is no single driver for the observed lake browning, but rather an interplay between different drivers varying in strength over time, such as afforestation, changes in areal use, declined S deposition, and increased temperature and precipitation.

Declaration of Competing Interest

The authors declare that there is no conflict of interest regarding the publication of this article.

Acknowledgements

This study was funded by Academy of Finland (Grant no. 295709; Y.X.) and it is also a delivery to the Nordic Centre of Excellence – Biowater (NordForsk project no. 82263). The laboratory and field work was funded by Norwegian University of Life Sciences (NMBU). The authors are grateful to Prof. Peter Dörsch (NMBU) for providing gas facilities during sediment DOM extraction. The authors are also grateful to Dr. Maria Potterf (UJ) for the help with plotting the catchment figure. The authors would like to thank Camilla Hagman (NMBU) for assisting with the extraction of long-term temperature and precipitation data. The authors would also like to thank Johnny Kristiansen (NMBU) and Trygve Fredriksen (NMBU) for the help during the measurements.

Appendix A. Supplementary data

Supplementary data to this article can be found online at https://doi.org/10.1016/j.scitotenv.2019.134388.

References

Anderson, N.J., Dietz, R.D., Engstrom, D.R., 2013. Land-use change, not climate, controls organic carbon burial in lakes. Proceedings. Biological Sciences 280, (1769). https://doi.org/10.1098/rspb.2013.1278 20131278.

Appleby, P.G., 2002. Chronostratigraphic techniques in recent sediments. In: Tracking Environmental Change Using Lake Sediments. Kluwer Academic Publishers, Dordrecht, pp. 171–203. https://doi.org/10.1007/0-306-47669-X_9.

Appleby, P.G., Oldfield, F., 1978. The calculation of lead-210 dates assuming a constant rate of supply of unsupported 210Pb to the sediment. CATENA 5 (1), 1–8. https://doi.org/10.1016/S0341-8162(78)80002-2.

Appleby, P.G., Nolan, P.J., Gifford, D.W., Godfrey, M.J., Oldfield, F., Anderson, N.J., Battarbee, R.W., 1986. 210Pb dating by low background gamma counting. Hydrobiologia 143 (1), 21–27. https://doi.org/10.1007/BF00026640.

Arvola, L., Rask, M., Ruuhijärvi, J., Tulonen, T., Vuorenmaa, J., Ruoho-Airola, T., Tulonen, J., 2010. Long-term patterns in pH and colour in small acidic boreal lakes of varying hydrological and landscape settings. Biogeochemistry 101 (1), 269–279. https://doi.org/10.1007/s10533-010-9473-y.

Attermeyer, K., Catalán, N., Einarsdottir, K., Freixa, A., Groeneveld, M., Hawkes, J.A., et al., 2018. Organic carbon processing during transport through boreal inland waters: particles as important sites. Journal of Geophysical Research: Biogeosciences 123 (8), 2412–2428. https://doi.org/10.1029/2018JG004500.

Bittar, T.B., Vieira, A.A.H., Stubbins, A., Mopper, K., 2015. Competition between photochemical and biological degradation of dissolved organic matter from the cyanobacteria Microcystis aeruginosa. Limnology 60, 1172–1194. https://doi.org/10.1002/lno.10090.

Bragée, P., Mazier, F., Nielsen, A.B., Rosén, P., Fredh, D., Broström, A., et al., 2015. Historical TOC concentration minima during peak sulfur deposition in two Swedish lakes. Biogeosciences 12 (2), 307–322. https://doi.org/10.5194/bg-12-307-2015.

Carpenter, S.R., Caraco, N.F., Correll, D.L., Howarth, R.W., Sharpley, A.N., Smith, V.H., 1998. Nonpoint pollution of surface waters with phosphorus and nitrogen. Ecol. Appl. 8 (3), 559–568. https://doi.org/10.2307/2641247.

Chen, M., Hur, J., 2015. Pre-treatments, characteristics, and biogeochemical dynamics of dissolved organic matter in sediments: a review. Water Res. 79, 10–25. https://doi.org/10.1016/j.watres.2015.04.018.

Chmiel, H.E., Niggemann, J., Kokic, J., Ferland, M.-È., Dittmar, T., Sobek, S., 2015. Uncoupled organic matter burial and quality in boreal lake sediments over the Holocene. Journal of Geophysical Research: Biogeosciences 120 (9), 1751–1763. https://doi.org/10.1002/2015JG002987.

Chow, A.T., Dahlgren, R.A., Harrison, J.A., 2007. Watershed sources of disinfection byproduct precursors in the Sacramento and San Joaquin Rivers, California. Environmental Science & Technology 41 (22), 7645–7652.

Cieslewicz, J., Gonet, S.S., 2004. Properties of humic acids as biomarkers of lake catchment management. Aquat. Sci. 66, 178–184. https://doi.org/10.1007/s00027-004-0702-0.

Coble, P.G., 2007. Marine optical biogeochemistry: the chemistry of ocean color. Chem. Rev. 107 (2), 402–418. https://doi.org/10.1021/cr050350+.

Cole, J.J., Prairie, Y.T., Caraco, N.F., McDowell, W.H., Tranvik, L.J., Striegl, R.G., et al., 2007a. Plumbing the global carbon cycle: integrating inland waters into the terrestrial carbon budget. Ecosystems 10 (1), 172–185. https://doi.org/10.1007/s10021-006-9013-8.

Cole, Jonathan J., Prairie, Y.T., Kortelainen, P., Sobek, S., Tranvik, L.J., Prairie, Y.T., et al., 2007b. Patterns and regulation of dissolved organic carbon: an analysis of 7,500 widely distributed lakes. Limnol. Oceanogr. 52 (3), 1208–1219. https://doi.org/10.4319/lo.2007.52.3.1208.

De Wit, H.A., Mulder, J., Hindar, A., Hole, L., 2007. Long-term increase in dissolved organic 364 carbon in streamwaters in Norway is response to reduced acid deposition. Environmental Science Technology 41, 7706–7713.

Dean, W.E., 1974. Determination of carbonate and organic matter in calcareous sediments and sedimentary rocks by loss on ignition: comparison with other methods. SEPM Journal of Sedimentary Research 44 (1), 242–248. https://doi.org/10.1306/74D729D2-2B21-11D7-8648000102C1865D.

Derrien, M., Lee, Y.K., Park, J.-E., Li, P., Chen, M., Lee, S.H., et al., 2017. Spectroscopic and molecular characterization of humic substances (HS) from soils and sediments in a watershed: comparative study of HS chemical fractions and the origins. Environ. Sci. Pollut. Res. 24 (20), 16933–16945. https://doi.org/10.1007/s11356-017-9225-9.

Derrien, M., Kim, M.-S., Ock, G., Hong, S., Cho, J., Shin, K.-H., Hur, J., 2018. Estimation of different source contributions to sediment organic matter in an agricultural-forested watershed using end member mixing analyses based on stable isotope ratios and fluorescence spectroscopy. Sci. Total Environ. 618, 569–578. https://doi.org/10.1016/J.SCITOTENV.2017.11.067.

Evans, A., Zelazny, L.W., Zipper, C.E., 1988. Solution parameters influencing dissolved organic carbon levels in three forest soils. Soil Sci. Soc. Am. J. 52 (6), 1789. https://doi.org/10.2136/sssaj1988.03615995005200060049x.

Evans, C.D., Jones, T.G., Burden, A., Ostle, N., Zieliński, P., Cooper, M.D.A., et al., 2012. Acidity controls on dissolved organic carbon mobility in organic soils. Glob. Chang. Biol. 18 (11), 3317–3331. https://doi.org/10.1111/j.1365-2486.2012.02794.x.

Finstad, A.G., Andersen, T., Larsen, S., Tominaga, K., Blumentrath, S., de Wit, H.A., et al., 2016. From greening to browning: catchment vegetation development and reduced S-deposition promote organic carbon load on decadal time scales in Nordic lakes. Sci. Rep. 6, (1). https://doi.org/10.1038/srep31944 31944.

Granhus, A., Hylen, G., Nilsen, J.-E.Ø., 2012. The Forest in Norway: Statistics of Forest Conditions and Resources in Norway. Norwegian Institute of Forestry and Landscape.

Guay, K.C., Beck, P.S.A., Berner, L.T., Goetz, S.J., Baccini, A., Buermann, W., 2014. Vegetation productivity patterns at high northern latitudes: a multi-sensor satellite data assessment. Glob. Chang. Biol. 20 (10), 3147–3158. https://doi.org/10.1111/gcb.12647.

Gudasz, C., Bastviken, D., Premke, K., Steger, K., Tranvik, L.J., 2012. Constrained microbial processing of allochthonous organic carbon in boreal lake sediments. Limnol. Oceanogr. 57 (1), 163–175. https://doi.org/10.4319/lo.2012.57.1.0163.

Guillemette, F., von Wachenfeldt, E., Kothawala, D.N., Bastviken, D., Tranvik, L.J., 2017. Preferential sequestration of terrestrial organic matter in boreal lake sediments. Journal of Geophysical Research: Biogeosciences 122 (4), 863–874. https://doi.org/10.1002/2016JG003735.

Guo, L., Macdonald, R.W., 2006. Source and transport of terrigenous organic matter in the upper Yukon River: evidence from isotope (δ13C, Δ 14C, and δ15N) composition of dissolved, colloidal, and particulate phases. Glob. Biogeochem. Cycles 20 (2), 1–12. https://doi.org/10.1029/2005GB002593.

Haaland, S., Hongve, D., Laudon, H., Riise, G., Vogt, R.D., 2010. Quantifying the drivers of the increasing colored organic matter in boreal surface waters. Environ. Sci. Technol. 44 (8), 2975–2980. https://doi.org/10.1021/es903179j.

Hagman, C.H.C., Ballot, A., Hjermann, D., Skjelbred, B., Brettum, P., Ptacnik, R., 2015. The occurrence and spread of Gonyostomum semen (Ehr.) Diesing (Raphidophyceae) in Norwegian lakes. Hydrobiologia 744 (1), 1–14. https://doi.org/10.1007/s10750-014-2050-y.

Håkanson, L., Jansson, M., 1983. Principles of Lake Sedimentology. Springer-Verlag, New York. Retrieved from https://inis.iaea.org/search/search.aspx?orig_q=RN:17050597.

Hansen, A.M., Kraus, T.E.C., Pellerin, B.A., Fleck, J.A., Downing, B.D., Bergamaschi, B. A., 2016. Optical properties of dissolved organic matter (DOM): effects of biological and photolytic degradation. Limnol. Oceanogr. 61 (3), 1015–1032. https://doi.org/10.1002/lno.10270.

Heiri, O., Lotter, A., Lemcke, G., 2001. Loss on ignition as a method for estimating organic and carbonate content in sediments. J. Paleolimnol. 25, 101–110. https://doi.org/10.1017/CBO9781107415324.004.

Helms, J.R., Stubbins, A., Ritchie, J.D., Minor, E.C., Kieber, D.J., Mopper, K., 2008. Absorption spectral slopes and slope ratios as indicators of molecular weight, source, and photobleaching of chromophoric dissolved organic matter. Limnol. Oceanogr. 53 (3), 955–969. https://doi.org/10.4319/lo.2008.53.3.0955.

Hongve, D., Åkesson, G., 1996. Spectrophotometric determination of water colour in Hazen units. Water Res. 30 (11), 2771–2775. https://doi.org/10.1016/S0043-1354(96)00163-7.

Hongve, D., Riise, G., Kristiansen, J.F., 2004. Increased colour and organic acid concentrations in Norwegian forest lakes and drinking water - a result of increased precipitation? Aquat. Sci. 66 (2), 231–238. https://doi.org/10.1007/s00027-004-0708-7.

Hur, J., Lee, B.M., Shin, K.H., 2014. Spectroscopic characterization of dissolved organic matter isolates from sediments and the association with phenanthrene binding affinity. Chemosphere 111, 450–457. https://doi.org/10.1016/j.chemosphere.2014.04.018.

Kalbitz, K., Solinger, S., Park, J.-H., Michalzik, B., Matzner, E., 2000. Controls on the dynamics of dissolved organic matter in soils: a review. Soil Sci. 165 (4), 277–304. https://doi.org/10.1097/00010694-200004000-00001.

Karlsson, J., Byström, P., Ask, J., Ask, P., Persson, L., Jansson, M., 2009. Light limitation of nutrient-poor lake ecosystems. Nature 460 (7254), 506–509. https://doi.org/10.1038/nature08179.

Knoll, L.B., Williamson, C.E., Pilla, R.M., Leach, T.H., Brentrup, J.A., Fisher, T.J., 2018. Browning-related oxygen depletion in an oligotrophic lake. Inland Waters 8 (3), 255–263. https://doi.org/10.1080/20442041.2018.1452355.

Köhler, S.J., Kothawala, D., Futter, M.N., Liungman, O., Tranvik, L., 2013. In-lake processes offset increased terrestrial inputs of dissolved organic carbon and color to lakes. PLoS One 8 (8), 1–12. https://doi.org/10.1371/journal.pone.0070598.

Kothawala, D.N., Stedmon, C.A., Muller, R.A., Weyhenmeyer, G.A., Köhler, S.J., Tranvik, L.J., 2014. Controls of dissolved organic matter quality: evidence from a large-scale boreal lake survey 20, 1101–1114. https://doi.org/10.1111/gcb.12488.

Kritzberg, E.S., 2017. Centennial-long trends of lake browning show major effect of afforestation. Limnology and Oceanography Letters 2 (4), 105–112. https://doi.org/10.1002/lol2.10041.

Kritzberg, E.S., Ekström, S.M., 2012. Increasing iron concentrations in surface waters - a factor behind brownification? Biogeosciences 9 (4), 1465–1478. https://doi.org/10.5194/bg-9-1465-2012.

Lambert, T., Teodoru, C.R., Nyoni, F.C., Bouillon, S., Darchambeau, F., Massicotte, P., Borges, A.V., 2016. Along-stream transport and transformation of dissolved organic matter in a large tropical river. Biogeosciences 13 (9), 2727–2741. https://doi.org/10.5194/bg-13-2727-2016.

Lapierre, J.-F., Del Giorgio, P.A., 2014. Partial coupling and differential regulation of biologically and photochemically labile dissolved organic carbon across boreal aquatic networks. Biogeosciences 11, 5969–5985. https://doi.org/10.5194/bg-11-5969-2014.

Li, P., Hur, J., 2017. Utilization of UV-Vis spectroscopy and related data analyses for dissolved organic matter (DOM) studies: a review. Crit. Rev. Environ. Sci. Technol. 47 (3), 131–154. https://doi.org/10.1080/10643389.2017.1309186.

Lie, O., 2002. Peat and Peat Use (in Norwegian). Våler Torvdriftsmuseum Foundation, p. 72.

Maerki, M., Müller, B., Wehrli, B., 2006. Microscale mineralization pathways in surface sediments: a chemical sensor study in Lake Baikal. Limnol. Oceanogr. 51 (3), 1342–1354. https://doi.org/10.4319/lo.2006.51.3.1342.

Meyer-Jacob, C., Michelutti, N., Paterson, A.M., Monteith, D., Yang, H., Weckström, J., et al., 2017. Inferring past trends in lake water organic carbon concentrations in northern lakes using sediment spectroscopy. Environ. Sci. Technol. 51 (22), 13248–13255. https://doi.org/10.1021/acs.est.7b03147.

Mielnik, L., Kowalczuk, P., 2018. Optical characteristic of humic acids from lake sediments by excitation-emission matrix fluorescence with PARAFAC model. J. Soils Sediments 18 (8), 2851–2862. https://doi.org/10.1007/s11368-018-1947-x.

Moldan, F., Cosby, B.J., Wright, R.F., 2013. Modeling past and future acidification of Swedish Lakes. AMBIO 42 (5), 577–586. https://doi.org/10.1007/s13280-012-0360-8.

Monteith, D.T., Stoddard, J.L., Evans, C.D., de Wit, H.A., Forsius, M., Høgåsen, T., et al., 2007. Dissolved organic carbon trends resulting from changes in atmospheric deposition chemistry. Nature 450 (7169), 537–540. https://doi.org/10.1038/nature06316.

Murphy, K.R., Stedmon, C.A., Graeber, D., Bro, R., 2013. Fluorescence spectroscopy and multi-way techniques. PARAFAC. Anal. Methods 5 (23), 6557. https://doi.org/10.1039/c3ay41160e.

Murphy, K.R., Stedmon, C.A., Wenig, P., Bro, R., 2014. OpenFluor– an online spectral library of auto-fluorescence by organic compounds in the environment. Anal. Methods 6 (3), 658–661. https://doi.org/10.1039/C3AY41935E.

Nelson, N.B., Siegel, D.A., 2013. The global distribution and dynamics of chromophoric dissolved organic matter. Annu. Rev. Mar. Sci. 5 (1), 447–476. https://doi.org/10.1146/annurev-marine-120710-100751.

Ohno, T., 2002. Fluorescence inner-filtering correction for determining the humification index of dissolved organic matter. Environmental Science & Technology 36 (4), 742–746. https://doi.org/10.1021/ES0155276.

Oni, S.K., Futter, M.N., Bishop, K., Köhler, S.J., Ottosson-Löfvenius, M., Laudon, H., 2013. Long-term patterns in dissolved organic carbon, major elements and trace metals in boreal headwater catchments: trends, mechanisms and heterogeneity. Biogeosciences 10. https://doi.org/10.5194/bg-10-2315-2013.

Peuravuori, J., Pihlaja, K., 1997. Molecular size distribution and spectroscopic properties of aquatic humic substances. Anal. Chim. Acta 337 (2), 133–149. https://doi.org/10.1016/S0003-2670(96)00412-6.

Pilla, R.M., Williamson, C.E., Zhang, J., Smyth, R.L., Lenters, J.D., Brentrup, J.A., et al., 2018. Browning-related decreases in water transparency lead to long-term increases in surface water temperature and thermal stratification in two small lakes. Journal of Geophysical Research: Biogeosciences 123 (5), 1651–1665. https://doi.org/10.1029/2017JG004321.

Renberg, I., Bigler, C., Bindler, Richard, Norberg, Matilda, Rydberg, Johan, Segerström, Ulf, 2009. Environmental history: a piece in the puzzle for establishing plans for environmental management. J. Environ. Manag. 90 (8), 2794–2800. https://doi.org/10.1016/J.JENVMAN.2009.03.008.

Rohrlack, T., & Haaland, S. (2017). Paleolimnological survey of Lundebyvannet in Eidsberg municipality (in Norwegian). *MINA Report 44*, 20 s.

Roulet, N., Moore, T.R., 2006. Browning the waters. Nature 444 (7117), 283–284. https://doi.org/10.1038/444283a.

Royston, P., 1995. Remark AS R94: a remark on algorithm AS 181: the W-test for normality. Appl. Stat. 44 (4), 547. https://doi.org/10.2307/2986146.

Santín, C., Yamashita, Y., Otero, X.L., Álvarez, M.Á., Jaffé, R., 2009. Characterizing humic substances from estuarine soils and sediments by excitation-emission matrix spectroscopy and parallel factor analysis. Biogeochemistry 96 (1–3), 131–147. https://doi.org/10.1007/s10533-009-9349-1.

Saulnier-Talbot, É., Saulnier-Talbot, & Émilie. (2016). Paleolimnology as a tool to achieve environmental sustainability in the anthropocene: an overview. Geosciences, 6(2), 26. doi:https://doi.org/10.3390/geosciences6020026.

Sobek, S., Durisch-Kaiser, E., Zurbrügg, R., Wongfun, N., Wessels, M., Pasche, N., Wehrli, B., 2009. Organic carbon burial efficiency in lake sediments controlled by oxygen exposure time and sediment source. Limnol. Oceanogr. 54 (6), 2243–2254. https://doi.org/10.4319/lo.2009.54.6.2243.

Soranno, P.A., Hubler, S.L., Carpenter, S.R., Lathrop, R.C., 1996. Phosphorus loads to surface waters: a simple model to account for spatial pattern of land use. Ecol. Appl. 6 (3), 865–878. https://doi.org/10.2307/2269490.

Stabbetorp, H., 2014. Agricultural developement since 1950. Utviklingstrekk av betydning for vannkvaliteten (in Norwegian). Vann 01, 89–96.

Stedmon, C.A., Markager, S., 2005. Resolving the variability in dissolved organic matter fluorescence in a temperate estuary and its catchment using PARAFAC analysis. Limnol. Oceanogr. 50 (2), 686–697. https://doi.org/10.4319/lo.2005.50.2.0686.

Stedmon, C.A., Markager, S., Bro, R., 2003. Tracing dissolved organic matter in aquatic environments using a new approach to fluorescence spectroscopy. Mar. Chem. 82 (3–4), 239–254. https://doi.org/10.1016/S0304-4203(03)00072-0.

Thrane, J.-E., Kyle, M., Striebel, M., Haande, S., Grung, M., Rohrlack, T., Andersen, T., 2015. Spectrophotometric analysis of pigments: a critical assessment of a high-

throughput method for analysis of algal pigment mixtures by spectral deconvolution. PLoS One 10, (9). https://doi.org/10.1371/journal.pone.0137645 e0137645.

Torres, I.C., Inglett, P.W., Brenner, M., Kenney, W.F., Reddy, K.R., 2012. Stable isotope (δ13 C and δ15 N) values of sediment organic matter in subtropical lakes of different trophic status. J. Paleolimnol. 47 (4). https://doi.org/10.1007/s10933-012-9593-6.

Tranvik, L.J., Downing, J.A., Cotner, J.B., Loiselle, S.A., Striegl, R.G., Ballatore, T.J., et al., 2009. Lakes and reservoirs as regulators of carbon cycling and climate. Limnol. Oceanogr. 54 (6part2), 2298–2314. https://doi.org/10.4319/lo.2009.54.6_part_2.2298.

Valinia, S., Futter, M.N., Cosby, B.J., Rosén, P., Fölster, J., 2015. Simple models to estimate historical and recent changes of total organic carbon concentrations in lakes. Environmental Science & Technology 49 (1), 386–394. https://doi.org/10.1021/es503170r.

Weyhenmeyer, G.A., Prairie, Y.T., Tranvik, L.J., 2014. Browning of boreal freshwaters coupled to carbon-iron interactions along the aquatic continuum. PLoS One 9 (2). https://doi.org/10.1371/journal.pone.0088104.

Wilson, H.F., Xenopoulos, M.A., 2009. Effects of agricultural land use on the composition of fluvial dissolved organic matter. Nat. Geosci. 2 (1), 37–41. https://doi.org/10.1038/ngeo391.

de Wit, H.A., Austnes, K., Hylen, G., Dalsgaard, L., 2015. A carbon balance of Norway: terrestrial and aquatic carbon fluxes. Biogeochemistry 123 (1–2), 147–173. https://doi.org/10.1007/s10533-014-0060-5.

Wolfe, A.P., Kaushal, S.S., Fulton, J.R., McKnight, D.M., 2002. Spectrofluorescence of sediment humic substances and historical changes of lacustrine organic matter provenance in response to atmospheric nutrient enrichment. Environmental Science & Technology 36 (15), 3217–3223.

Yamashita, Y., Lu, C.-J., Ogawa, H., Nishioka, J., Obata, H., Saito, H., 2015. Application of an in situ fluorometer to determine the distribution of fluorescent organic matter in the open ocean. Mar. Chem. 177, 298–305. https://doi.org/10.1016/J.MARCHEM.2015.06.025.

Yu, B., Dong, H., Jiang, H., Lv, G., Eberl, D., Li, S., Kim, J., 2009. The role of clay minerals in the preservation of organic matter in sediments of Qinghai lake, NW China. Clay Clay Miner. 57 (2), 213–226. https://doi.org/10.1346/CCMN.2009.0570208.

Zhang, Y., van Dijk, M.A., Liu, M., Zhu, G., Qin, B., 2009. The contribution of phytoplankton degradation to chromophoric dissolved organic matter (CDOM) in eutrophic shallow lakes: field and experimental evidence. Water Res. 43 (18), 4685–4697. https://doi.org/10.1016/j.watres.2009.07.024.

Zhou, Y., Zhang, Y., Jeppesen, E., Murphy, K.R., Shi, K., Liu, M., et al., 2016. Inflow rate-driven changes in the composition and dynamics of chromophoric dissolved organic matter in a large drinking water lake. Water Res. 100, 211–221. https://doi.org/10.1016/j.watres.2016.05.021.